Supporting Material for "Alpha-phase synchrony for multiresistant chronic low back pain patients: an open-label pilot study"

Online EEG data processing for NFB training sessions

DATA PRE-PROCESSING

Pre-processing treatment were built using Mensia's proprietary algorithms as implemented in the NeuroRT software platform (v2, Mensia Technologies, Paris, France), which runs the real-time core of NeuroRT Training. The EEG signals were band-pass filtered using a 1-45Hz 1st-order Butterworth filter, and band –stop filtered in the frequency range 47-53 Hz with a 3rd-order Butterworth notch filter to suppress 50Hz power line interference.

BLIND SOURCE SEPARATION FOR EYE BLINK CORRECTION

A primary source of physiological noise in EEG signals is that of eye movements and particularly eye blinks, which typically generate very large amplitude artefacts. Because of their amplitude and spectral content, which may overlap with the alpha activity we are meaning to train in our protocol, it is desirable to remove such signal by means of source separation techniques.

In blind source separation (BSS) we assume that the observed recordings at the scalp are the result of an unknown mixture of unknown sources [6] [9]. Because of a number of physiological and physical reasons listed in [12], the multichannel EEG signal recorded at N channels/sensors $X \in \mathbb{R}^N$ can be modeled as a linear (instantaneous) combination of $M \leq N$ independent sources $S \in \mathbb{R}^M$, such as:

$$X = A\,S\,,$$

where $A \in R^{N \times M}$ is the mixing matrix, considered constant throughout the recording. The goal of BSS is to estimate the separating/demixing matrix $B \in \mathbb{R}^{M \times N}$ allowing source estimation:

$$S = B\,X\,,$$

with B being the estimated pseudo-inverse of (unknown) matrix A. Sources are estimated up to a permutation and scaling factor. Many methods exist to estimate this separating matrix, including independent component analysis (ICA) [8], which is based on the estimation of higher order statistics (HOS) [5], and methods based on second order statistics (SOS) [4]. The cleaned signal is obtained by rejecting sources identified as artifacts thanks to a diagonal activation matrix $D \in \mathbb{R}^{M \times M}$ containing 0 for artifact components and 1 otherwise:

$$\tilde{X} = A\,D\,S\,.$$

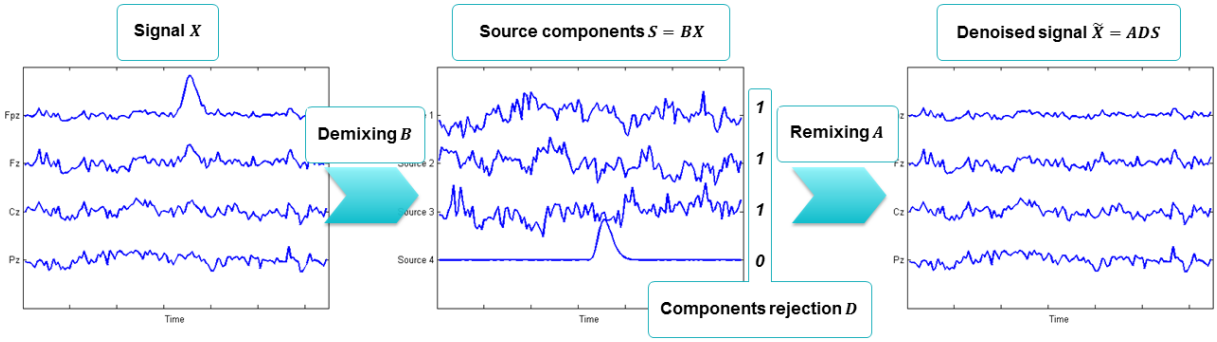

Figure SM1: Illustration of the blind source separation denoising: the EEG signal (left) is decomposed in sources components (middle), and once artefactual sources rejected, the signal is projected back into the sensor space, giving the denoised signal (right).

The process of denoising by BSS is summarized schematically in Figure SM1. Note that we have implemented an unsupervised online eye-blinks denoising procedure that does not make use of EOG traces, nor a training database. It is reference-free, *i.e.* it does not need spatial or temporal templates, which are dependent from the headset and thus potentially specific to the training subject(s). Therefore, this generic method is compatible with any headset. In order to achieve this, we allow only a non-supervised self-calibration step, *i.e.*, a small segment of signal can be used to learn relevant features. Consequently, this type of denoising can be applied on a single signal/trial, as well as on a complete database. The technique was validated on large database showing increased signal to noise ratios (SNR) on both spectral and temporal physiologically meaningful endpoints [3].

RIEMANNIAN GEOMETRY FOR ARTIFACT DETECTION AND SIGNAL QUALITY INDEX

In this framework, covariance matrices are used as descriptors of EEG signals so that every epoch of EEG signal is represented by its spatial covariance matrix Σ. For the filtered EEG signal $X \in \mathbb{R}^{N \times T}$ recorded at N channels during T samples, the spatial covariance matrix is estimated as:

$$\Sigma = \frac{1}{T-1} X^T X \, .$$

Covariance matrices naturally live in a Riemannian manifold, thus appropriate tools of Riemannian geometry should be applied to computes distances between covariance matrices [11]. An average covariance matrix $\bar{\Sigma}$ can then always be estimated and used as a reference representing a baseline activity. Such baseline activity can be clean EEG data of one subject as well as average clean EEG data across a sample recorded under homogeneous conditions.

The Riemannian distance between the current matrix Σ and the reference $\bar{\Sigma}$ is defined by:

$$d(\Sigma, \bar{\Sigma}) = \left[\sum_{n=1}^{N} \log^2 \lambda_n(\Sigma, \bar{\Sigma}) \right]^{\frac{1}{2}}$$

where λ_n are the the eigenvalues of $\Sigma^{-1/2} \bar{\Sigma} \Sigma^{-1/2}$ [16].

Riemannian geometry is used to target artefactual epochs of signal. Pre-processed EEG signals are segmented into 0.25s-overlapping epochs of 2s and represented by their spatial covariance matrix Σ. Then the average $\bar{\Sigma}$ of clean epochs per subjects is computed and the distance $d(\Sigma, \bar{\Sigma})$ between the current matrix Σ and the average $\bar{\Sigma}$ is standardized and compared to a threshold. A z-score threshold of 2.5 is chosen to reject artefactual epochs.

Called Riemannian potato [1] [2], this method is applied online to ensure that no artefactual EEG data is used during the active conditioning process.

After online preprocessing and denoising, the application extracts neuromarker and rewards the user according to the specified protocol.

ALPHA SYNCHRONY (APS) AND CONCENTRATION (APC) NEUROMARKER EXTRACTION

Pre-processed EEG data that was deemed of sufficient quality was used to extract an alpha phase synchrony (APS) neuromarker [15], which was fed back to the user in real time. Signals were band-pass filtered between 8 and 12Hz using a 5th order Butterworth filter. These filtered signals are then spatially averaged over all channels. Then, a moving average on a window of 2s every 0.25s was used to compute the Frobenius squared norm of the average as a proxy for alpha synchrony power, called a. Finally, this metric is normalized by the global field power of pre-processed signals, computed similarly with a moving average on a window of 2s every 0.25s used to compute the Frobenius squared norm, called b. Normalization of the neuromarker is given by:

$$\mathrm{APS} = log(\varepsilon + a) \,/\, log\,(\varepsilon + b),$$

with ε=1.1.

To study these different levels of changes, the entire dataset was post-processed to extract the evolution of two pre-specified neuromarkers: the APS defined above, sensitive to both amplitude and phase which was trained, and the alpha phase concentration (APC) [14] [7] solely sensitive to phase and arguably relating more specifically to the modulation of the nucleus accumbens [13], which we believe relates more specifically to the symptoms of chronic pain and their evolution.

For the extraction of alpha phase concentration [7], Fourier Transform is computed after a Hamming window of 1s every 0.25s. Fourier coefficients are averaged between 8 and 12Hz, and this averaged complex coefficient is then normalized (absolute value equal to 1). The normalized coefficients are averaged over all channels, and finally, we keep the absolute value of this average:

$$\mathrm{APC} = \left| \frac{1}{N} \sum_{n=1}^{N} e^{i\,\varphi_n} \right|,$$

where φ_n is the phase of alpha band in channel n. This metric is also known as circular mean resultant length [14], inter-trial phase coherence, inter-trial phase clustering or phase coherence [7] [10].

AUTOMATED THRESHOLDING OF THE NEUROMARKER

In order to provide efficient neurofeedback training, i.e. to enable the subject to gain control of the brain activity and to train it in the desired direction, the threshold between a positive and negative reward must be finely tuned. Indeed, threshold adjustment stimulates the subjects and maintains engagement to the session.

The actual clinical practice of neurofeedback supposes trainer supervision with manual selection of the threshold during the session. Consequently, neurofeedback sessions have to be performed by the subject with assistance of a trained specialist. Said supervision considerably limits availability of neurofeedback sessions. Moreover, it also limits feasibility studies and repeatability.

To avoid these limitations, an unsupervised automatic adjustment of the threshold has been implemented, estimating a piece-wise constant threshold based on the distribution of the neuromarker computed on a sliding window [17], and is illustrated in Figure SM2.

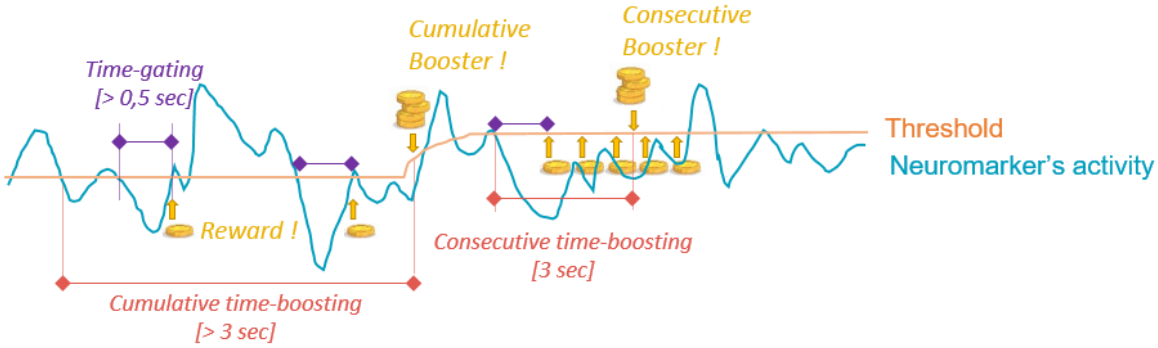

Figure SM2: Illustration of the automated thresholding. The brain activity of interest extracted from the EEG activity (neuromarker) is represented in blue line. It oscillates around a threshold (orange line), constant and adaptive during the session. The discrete feedback (here "Reward!") is displayed to users when the neuromarker activity is maintained below the threshold (for a down training protocol) for more than 0.5 seconds (time-gating). A positive reinforcement (here "Cumulative Booster!") is showed to the user when the neuromarker activity is maintained below the threshold (for a down training protocol) during more than 3 seconds (time-boosting). If the three seconds are reached consecutively, a "Consecutive Booster" is earned. This way we promote a reinforcement and a maintenance in time of this activity.

REFERENCES

[1] A Barachant, A Andreev, and M Congedo. The Riemannian Potato: an automatic and adaptive artifact detection method for online experiments using Riemannian geometry. In *Proc. TOBI Workshop IV*, pages 19–20, 2013.

[2] Q. Barthélemy, L. Mayaud, D. Ojeda, and M. Congedo. The Riemannian potato field: a tool for online signal quality index of EEG. *IEEE Trans Neural Syst Rehabil Eng*, 27:244–255, 2019.

[3] Q. Barthélemy, L. Mayaud, Y. Renard, D. Kim, S.W. Kang, J. Gunkelman, and M. Congedo. Online denoising of eye-blinks in electroencephalography. *Neurophysiol Clin*, 47:371–391, 2017.

[4] A. Belouchrani, K. Abed-Meraim, J. Cardoso, and E. Moulines. A blind source separation technique using second-order statistics. *IEEE Trans Signal Process*, 45:434–444, 1997.

[5] J.F. Cardoso and A. Souloumiac. Blind beamforming for non-Gaussian signals. *IEE Proceedings F - Radar and Signal Processing*, 140:362–370, 1993.

[6] A. Cichocki and S. Amari. *Adaptive Blind Signal and Image Processing : Learning Algorithms and Applications*. John Wiley & Sons, 2003.

[7] M X Cohen. *Analyzing neural time series data: theory and practice*. MIT press, 2014.

[8] P. Comon. Independent Component Analysis, a new concept ? *Signal Process*, 36:287–314, 1994.

[9] P. Comon and C. Jutten. *Handbook of Blind Source Separation, Independent Component Analysis and Applications*. New York: Academic, 2010.

[10] M. Congedo. Non-parametric synchronization measures used in EEG and MEG. Technical report, GIPSA-lab, CNRS, University Grenoble Alpes, Grenoble-INP, 2018.

[11] M. Congedo, A. Barachant, and R. Bhatia. Riemannian geometry for EEG-based brain-computer interfaces; a primer and a review. *Brain Comput Interfaces*, 4:1–20, 2017.

[12] M. Congedo, C. Gouy-Pailler, and C. Jutten. On the blind source separation of human electroencephalogram by approximate joint diagonalization of second order statistics. *Clin Neurophysiol*, 119:2677–2686, 2008.

[13] J M Horschig, R Smolders, M Bonnefond, J-M Schoffelen, P Van den Munckhof, P R Schuurman, R Cools, D Denys, and O Jensen. Directed communication between nucleus accumbens and neocortex in humans is differentially supported by synchronization in the theta and alpha band. *PloS One*, 10(9):e0138685, 2015.

[14] K V Mardia. *Statistics of directional data*. Academic press, 1972.

[15] JT McKnight and LG Fehmi. Attention and neurofeedback synchrony training: Clinical results and their significance. *J Neurother*, 5:45–61, 2001.

[16] M Moakher. A differential geometric approach to the geometric mean of symmetric positive-definite matrices. *SIAM J Matrix Anal Appl*, 26(3):735–747, 2005.

[17] M. Prat and L. Mayaud. Automated thresholding for unsupervised neurofeedback sessions, 2017.